

Contract No.:

This manuscript has been authored by Savannah River Nuclear Solutions (SRNS), LLC under Contract No. DE-AC09-08SR22470 with the U.S. Department of Energy (DOE) Office of Environmental Management (EM).

Disclaimer:

The United States Government retains and the publisher, by accepting this article for publication, acknowledges that the United States Government retains a non-exclusive, paid-up, irrevocable, worldwide license to publish or reproduce the published form of this work, or allow others to do so, for United States Government purposes.

METHOD FOR ESTIMATING THE DENSITY OF HIGH LEVEL NUCLEAR WASTE GLASS

CORY L. TRIVELPIECE^{1*}, THOMAS B. EDWARDS¹, FABIENNE C. JOHNSON¹, KIMBERLY P. CRAPSE¹, KEVIN M. FOX¹

ABSTRACT:

A database of over 1100 silicate glass compositions and densities was compiled and used to evaluate the efficacy of an algorithm for estimating the density of silicate glass compositions. We sought to develop a parsimonious algorithm based on the additivity of partial molar volumes of individual oxide components weighted by their mole fraction in a glass composition. Bound molar volumes were used for oxides in which the density of the oxide bound in a glass matrix was previously determined. The bound molar volumes were known for oxides covering 97.5 mole percent of the database compositional space. The measured glass densities were plotted against the estimated glass densities and a linear regression yielded an $R^2_{\text{adj.}} = 0.95$ and a slope and intercept of approximately one and zero, respectively. This regression suggests that glass densities estimated by the algorithm, within analysis uncertainty, are equal to the measured densities of the glasses. In addition to the development of the density estimation, we corroborated many of the referenced bound molar volume data used in the parameterization of the estimation algorithm via linear regression of the individual partial molar volumes versus the inverse measured densities (specific volumes) of the glasses in the database.

1. INTRODUCTION:

The waste loading and amount of fissile material in a high-level nuclear waste (HLW) glass is carefully controlled and typically must meet limits imposed by regulatory agencies for acceptance into permanent storage locations. Glass density is affected by the amount of waste and/or fissile mass concentration that is allowable in an HLW glass canister¹⁻⁸. At the Savannah River Site, the Savannah River National Laboratory currently measures the densities of glasses as part of a “variability study” designed to determine the

* Corresponding author: cory.trivelpiece@srnl.doe.gov

1. Environmental, Materials, and Energy Sciences - Savannah River National Laboratory, Aiken, SC 29808

bounding limits for glass composition for an individual sludge batch. These measurements are coupled with other data to determine an upper limit density limit for a particular “sludge batch” to be processed by DWPF.

Efforts have been made in the past to estimate the density of a HLW glass based on its composition⁹⁻¹¹. What sets this current effort apart, is the reliance on additive properties combined with partial molar volumes for bound oxides in glasses that cover a large portion of the parameterization necessary to execute the estimation algorithm. We used a set of bound oxide partial molar volume data that was acquired by A.A. Appen¹² and summarized by M.B. Volf¹³ and glass compositions from multiple sources to achieve the results in this study. Importantly, there is no regression of measured versus estimated density data nor empirical “fitting” of data to achieve the final estimated density values. The method employed and described in this work correctly estimates, within stated statistical uncertainties, the density of a glass based on the glass’s composition. The resulting algorithm provides researchers, engineers, and plant operators with an intuitive tool for estimating glass density.

2. EXPERIMENTAL PROCEDURE:

2.1 DATABASE DEVELOPMENT

The database employed in this study¹⁴ was compiled from multiple sources including: Defense Waste Processing Facility (DWPF) glass variability studies with experimental work performed at Savannah River National Laboratory (SRNL) or at the Vitreous State Laboratory (VSL) at Catholic University of America; HLW studies conducted at Pacific Northwest National Laboratory (PNNL); and numerous literature sources. The database contains 1104 unique glass compositions – 329 of these are variants of HLW glass compositions, and an additional 148 glasses are taken from sources related to nuclear waste glass studies^{1-6, 10, 15-34}. The remainder of the glasses in database range from simple binary compositions to more complex systems that contain up to ten oxide components.

The database covers measured glass density ranges from 2.224 g/cm³ to 3.997 g/cm³. [Figure 1](#) shows the compositional coverage for each oxide and estimates the numbers of glasses containing each oxide. The complexity of the glasses in the database in terms of number of oxide components varies between binary compositions and HLW compositions containing as many as 26 individual oxides.

2.2 CALCULATIONS

Initially, the specific volumes of the glass compositions were estimated by summing the partial molar volumes weighted by mole fraction of the various oxide components in the glass as demonstrated by Equation 1.

$$V_E = \frac{\sum x_i V_i}{M_{glass}} \quad (1)$$

$$M_{glass} = \sum x_i m_i \quad (2)$$

Where: V_E is the specific volume of the glass (cm³/g), M_{glass} is the molar mass of the glass (g/mol), defined in Equation 2, x_i is the mole fraction of the i^{th} oxide component of the glass, V_i is the partial molar volume of the i^{th} oxide component, and m_i is the molar mass of the oxide (g/mol). The estimated density is then the reciprocal of the specific volume (Equation 3):

$$\rho_E = \frac{1}{V_E} \quad (3)$$

Where, ρ_E is the estimated glass density (g/cm³).

We included an uncertainty, perhaps more appropriately “error,” in the estimation via an additional term, ϵ , on both sides of Equation 3, which reflects the fact that this evaluation relies upon measurements (e.g., glass composition analysis) with intrinsic uncertainties. We assumed that the errors associated with the

estimated densities were normally distributed such that the error is equal to the standard deviation of the estimates' residuals as shown in Equation 4.

$$\epsilon = s (\rho_{measured} - \rho_E) \quad (4)$$

Where s is the standard deviation of the residual estimates, $\rho_{measured}$ is the measured glass density, and ρ_E is the estimated glass density so that the estimated density and associated error for an individual glass composition are determined from Equation 5:

$$\rho_E = \left(\frac{1}{V_E} \right) + \epsilon = \frac{M_{glass}}{\sum x_i V_i} + \epsilon \quad (5)$$

2.3 ASSUMPTIONS

The following assumptions were employed with respect to composition, elemental speciation, and oxide partitioning for the glasses in the database utilized in this study.

1. We assumed that any sulfur species present in the glasses, a common occurrence in HLW compositions and usually presented as SO_3 or SO_4 , formed part of the glass matrix as Na_2SO_4 ³⁵. Given the typically low concentration of sulfur species present in HLW glass (<2 wt.%), this assumption was determined to have no effect on the applicability of the algorithm to estimate density within the bounds of our imposed uncertainty (Section 2.2). That being said, the input parameters and species partitioning can be amended to reflect new insights into sulfur/glass interactions; however, our current understanding of sulfur loading indicates that 2 wt.% is near the maximum amount of SO_x that can be incorporated homogeneously into glass^{36, 37}.
2. A small subset of HLW glasses contains elemental F and Se¹⁶. We assumed that F behaves as being loosely bonded to SiO_4 and AlO_4 tetrahedra³⁸⁻⁴² and does not have a large effect on the specific volume of the glass when present in these small quantities. Because of the large range of values

reported for various F species in glasses in the referenced literature, we flexed the algorithm by varying the partial molar volume of fluorine in the glass from 5 – 20 cm³/mol. The results of this exercise demonstrated that a large uncertainty in the F partial molar volume has immeasurable impact on the estimated densities for the glass compositions containing F in the database relative to the imposed uncertainty limit. Based on references ^{43,44}, we assumed that Se, when incorporated into the silicate glasses, resembled the structure of SeO₃²⁻.

3. The concentration of U-bearing oxides was partitioned between UO₂ and UO₃ in the glasses that contained uranium as suggested by Volf ⁴⁵. Uranium can exist in many oxidation states in a glass system depending on the reduction/oxidation (REDOX) environment of the melt as well as the coordination of other glass constituents. In terms of this work, we assumed, based on the suggestion by Volf and others, that any U in the glasses reported as U₃O₈ was divided between UO₂ and UO₃ accordingly: U₃O₈ = UO₂·2UO₃. As with other low-concentration glass constituents, variability in the U-speciation did not impact the efficacy of the algorithm in estimating glass density within the limits we imposed.

Other assumptions, such as the additivity of the partial molar volumes of oxide components in glass, were taken as valid for the purpose of this work. Effects such as those associated with varying B and Al speciation and the thermal history of the glasses were assumed to be negligible insofar as their influence on the density estimation can be absorbed by our applied uncertainty. Any effects associated with the non-ideality of a glass versus crystal of the same composition were assumed to be similarly negligible as is borne out by the accuracy of the estimations which will be described.

2.4 PARTIAL MOLAR VOLUMES

In developing the database and the various parameters needed to estimate the densities of the glasses contained in the database, the idea of utilizing “bound molar volumes” and “bound oxide densities” was

employed. As noted by Volf ¹³, “*the volume of melted glass is smaller than the sum of the volumes of free oxides.*” In this context, the phrase “free oxides” is referencing the stand-alone volume of a glass oxide component whereas “bound molar volume” or “bound oxide density” refers to the property of an oxide component when incorporated into a glass matrix.

Indeed, there is measured and reported variability between the free oxide and bound oxide densities and molar volumes for a number of major oxides contained in HLW glass formulations. Table 1 gives the partial molar volumes of all oxides parameterized in the database, and the values from Volf ¹³ are especially delineated to highlight their variability from the “free oxide molar volume”.

Inspection of Table 1 reveals no ostensible correlation between the oxide properties and ratio of the bound oxide density to the free oxide density. That is to say, some oxides have a greater bound molar volume than free molar volume, while others do not, and there is no clear macroscopic, property-based trend as to why this occurs. As such, no statistical correlation between the free vs. bound oxide densities, and the macroscopic physical properties of the oxides could be established (e.g., linear regression, extrapolation). Also observable from Table 1 is the fact that several oxides composing some of the glasses in the database do not have bound densities listed (e.g., Fe_2O_3 , U_3O_8). In such instances, we employed the free oxide density given by the Handbook of Chemistry and Physics ⁴⁶ as sufficient to estimate the density of all the glass compositions in the database. The rationale for this application is that the total number of moles of oxides in the database with “known” bound densities accounts for 97.5% of the total number of moles of oxides in the database. In terms of weight percent, the mass of oxides with a “known” bound density accounts for 95.7% of the entire mass of glass represented by the compositions in the database. While not insignificant, the amount of glass for which the bound density is unknown is sufficiently small enough to not affect the accuracy of the algorithm as was demonstrated by the results of the overall effort.

3.0 RESULTS AND DISCUSSION

The specific volumes of the glasses in the database were treated as a thermodynamically ideal, extensive, additive property. Accordingly, data from Table 1¹³ were combined with the compositions of the glasses from the database to generate a specific volume for each glass. These estimated specific volumes were plotted against the reciprocal of the measured density for each glass. The corresponding plot, along with a linear regression of these data and the associated 95% tolerance intervals are shown in [Figure 2a](#). A linear regression of the estimated specific volume versus the inverse measured density yielded a fit equation with a slope of approximately one and an intercept of approximately zero. When this line was extended through the origin of [Figure 2a](#), as shown in [Figure 2b](#), we observed that a slope and intercept of one and zero, respectively, are contained within the 95% confidence intervals of the individual predictions via the regression. In other words, the estimated specific volume is approximately equal to the inverse measured density of the glasses.

Similarly, the slope and intercept of the of the measured density versus the reciprocal of the estimated specific volume, or the estimated density, were also approximately one and zero, respectively. The relationship between the measured and estimated density along with the regression data are shown in [Figure 3](#). The upper and lower 95% tolerance intervals determined assuming a normal distribution of the prediction residuals are also shown in Figure 3. Again, an extension of the fit through the origin of the plot in Figure 3 demonstrates that the confidence intervals capture the origin serving as another indication of the accuracy of the density estimation via the weighted partial molar volumes of the oxides.

Analysis of the residuals of the estimates versus the measured densities indicates a slightly overpredicted bias. Viz., the mean of the residuals is slightly negative ($\mu = -0.0073$). This overprediction of the density, while not ideal, does provide for a layer of conservatism when estimating HLW glass density. A histogram

of the residuals along with the assumed normal distribution used for the establishing the 95% tolerance limits in Section 2.2 is shown in [Figure 4](#).

3.1 ESTIMATES OF HLW GLASS DENSITIES

The initial focus of this work was to establish a method by which the densities of potential HLW glass compositions could be estimated^{19-23, 47, 48}. The estimation algorithm and parameterization presented here is also applicable to any facility producing glass and gives operators an *a priori* method for determining glass densities without the need for measurement.

We evaluated the density estimations provided by Equation 3 against the measured values for a subset of glasses from the database that contained density values obtained by various institutions for simulated HLW glass compositions. The results of this evaluation are shown in Figure 5. Fourteen of the HLW compositions fall outside of the two-sided tolerance interval shown in Figure 5, which is approximately 4.3% of the glasses and expected for the subset of 329 glasses within the applied tolerances.

3.2 REGRESSION OF PARTIAL MOLAR VOLUMES

Not all of the oxides contained within the database have known partial molar volumes as discussed in Section 2.4. We attempted several methods of regression to delineate more accurate parameters for these “unknown” oxides. Our first effort was to substitute Equation 2 into Equation 1 such that the result could be expressed as:

$$\left(\frac{1}{\rho}\right) = \sum \frac{x_i}{M_{glass}} v_i + \epsilon = \sum x'_i v_i + \epsilon \quad (6)$$

Where x'_i is the known composition term and v_i may be allowed to play the role of the unknown coefficient representing the effect of oxide “i” in the relationship defined by Equation 6. This regression yielded mixed results. For the oxides in which the partial molar volume was known via Volf¹³, many of the

estimated partial molar volumes were close to the values given in Table 1. A comparison of the values from Table 1 to the estimated partial molar volumes is shown in [Figure 6](#). The estimated values for Bi_2O_3 , Sb_2O_3 , and ThO_2 (Figure 6 inset) were unrealistic (e.g., the estimated partial molar volume of Sb_2O_3 was $-53.34 \text{ cm}^3/\text{mol}$). However, for oxides that comprise a majority of the glass compositions in the database, the estimated partial molar volumes were similar to those reported in Table 1.

An additional method, in which individual partial molar volumes were isolated and estimated by solving Equation 1 for the individual molar volume of a specific oxide, also yielded mixed results, but did not improve upon the estimations beyond what was achievable with the values from Table 1. Ultimately, we decided to utilize the original set of literature-referenced partial molar volumes. However, we envision utilizing a larger data set in the future from which we can isolate glass subsets containing glasses for which the bound molar volumes are unknown and can then perform these regressions to improve our estimation parameterization.

4.0 CONCLUSIONS

Calculating the specific volume, and consequently density, of a glass composition via the partial molar volumes of the individual oxide components yielded estimates that were approximately equal to the measured values. This new look at a classic theory demonstrated that for certain industrial applications and processes, using composition-weighted, partial molar volumes to determine a glass density is sufficiently accurate to provide *a priori* estimates of a composition's density. We attempted to delineate the partial molar volumes of oxides in the database for which we did not have "bound" values. The results of this exercise were mixed: the estimated partial molar volumes agreed for several oxides for which the bound molar volume was already known; however, the estimates for many oxides (with known, i.e., in Table 1, and unknown bound values) were unrealistic. Upon further inspection, we observed that a degree of compositional leverage is required to determine an accurate partial molar volume via

regression. For instance, if the minimum and maximum concentrations of an oxide in the regression test set are separated by only a few percent, it is difficult to acquire a reasonable estimate of the effects of that oxide's molar volume on the overall specific volume of a glass. We intend to improve the parameterization in the future by utilizing larger datasets with more compositional leverage from which we can determine bound partial molar volumes for the "unknown" oxides. That being said, the algorithm and parameter set developed in this work are adequate for estimating HLW glass density.

5.0 Acknowledgements

Preparation of this manuscript was supported by the U.S. Department of Energy Office of River Protection Waste Treatment & Immobilization Plant Project, under the direction of Albert Kruger. Savannah River National Laboratory is operated by Savannah River Nuclear Solutions for the U.S. Department of Energy under contract number DE-AC09-08SR22470.

REFERENCES:

1. Edwards T, Johnson F, Kot W, Gan H, Pegg I. Evaluation of Glass Density to Support the Estimation of Fissile Mass Loadings from Iron Concentrations in SB9 Glasses. 2016 SRNL-TR-2016-00071, Rev. 0.
2. Edwards T, Peeler D, Kot W, Gan H, Pegg I. Evaluation of Glass Density to Support the Estimation of Fissile Mass Loadings from Iron Concentrations in SB8 Glasses. 2013 SRNL-STI-2013-00212, Rev. 0.
3. Edwards T, Peeler D. Evaluation of Glass Density to Support the Estimation of Fissile Mass Loadings from Iron Concentrations in SB7b Glasses. 2012 SRNL-STI-2012-00007, Rev. 0.
4. Edwards T, Peeler D. Evaluation of Glass Density to Support the Estimation of Fissile Mass Loadings from Iron Concentrations in SB7a Glasses. 2011 SRNL-STI-2011-00512, Rev. 0.
5. Edwards T, Peeler D. Evaluation of Glass Density to Support the Estimation of Fissile Mass Loadings from Iron Concentrations in SB6 Glasses. 2010 SRNL-STI-2010-00757, Rev. 0.
6. Edwards T, Peeler D. Estimation of Fissile Mass Loadings from Iron Concentrations in SB5 Glasses. 2009 SRNL-TR-2009-00258, Rev.0.
7. Hrma P, Crum JV, Bates DJ, Bredt PR, Greenwood LR, Smith HD. Vitrification and testing of a Hanford high-level waste sample. Part 1: Glass fabrication, and chemical and radiochemical analysis. *Journal of Nuclear Materials*. 2005;345(1):19-30.
8. Perez Jr JM, Bickford DF, Day DE, Kim D-S, Lambert SL, Marra SL, et al. High-level waste melter study report. Pacific Northwest National Laboratory, 2001 PNNL-13582.
9. Schumacher R. DWPF Batch 1, Waste Glass Investigations. 1991 WSRC-MS-90-348 WSRC-MS-90-348.

10. Schumacher R. Basic Data Report: Simulated New Batch 1 Glasses. 1998 WSRC-RP-95-0539 WSRC-RP-95-0539, Rev. 0.
11. Fluegel A. Global Model for Calculating Room-Temperature Glass Density from the Composition. *Journal of the American Ceramic Society*. 2007;90(8):2622-5.
12. Appen A. *Chemistry of Glass*. Leningrad, USSR: Khimiya Publishing House; 1970.
13. Volf M. *Mathematical Approach to Glass*. Amsterdam Elsevier Science Publishing Company, Inc.; 1988.
14. Trivelpiece C, Edwards T. Composition-based Density Model for High Level Waste Glasses. Savannah River National Laboratory, 2019 SRNL-STI-2018-00599.
15. Parkinson B, Holland D, Smith M, Howes A, Scales C. The effect of Cs₂O additions on HLW wasteform glasses. *Journal of Non-Crystalline Solids*. 2005;351(30-32):2425-32.
16. Shelby J. Appendix I. In: Seward III T, Vascott T, editors. *High Temperature Glass Melt Property Database for Process Modelling*. Westerville, OH: The American Ceramic Society; 2005. p. 261-74.
17. Schumacher R. DWPF Batch 1, Waste Glass Investigations. 1990 WSRC-MS-90-348 WSRC-MS-90-348.
18. Morey G. *Properties of Glass*. New York, NY: Reinhold Publishing Corporation; 1938.
19. Kot W, Pegg I, Johnson F, Edwards T. Final Report Sludge Batch 9 Variability Study with Frit 803. Vitreous State Laboratory, 2016 VSL-16R3370-1, Rev. 0.
20. Kot W, Pegg I, Peeler D, Edwards T. Final Report Sludge Batch 8 Variability Study with Frit 803. Vitreous State Laboratory, 2013 VSL-13R2580-1, Rev. 0.
21. Johnson F, Edwards T. Sludge Batch 7b Glass Variability Study. Savannah River National Laboratory, 2011 SRNL-STI-2011-00440, Rev. 0.
22. Peeler D, Edwards T. The Sludge Batch 7a Glass Variability Study with Frit 418 and Frit 702. Savannah River National Laboratory, 2011 SRNL-STI-2011-00063, Rev. 0.
23. Johnson F, Edwards T. Sludge Batch 6 Variability Study with Frit 418. Savannah River National Laboratory, 2010 SRNL-STI-2010-00242, Rev. 0.
24. Kot W, Pegg I. Measurements of Glass Density and Melt Viscosity to Support Salt Waste Processing Facility (SWPF) Gap Analysis Study. 2016 VSL-15L3500-2, Rev. 1.
25. Vienna J, Hirma P, Jiricka A, Smith D, Lorier T, Reamer I, et al. Hanford Immobilized LAW Product Acceptance Testing: Tanks Focus Area Results. Pacific Northwest National Lab., 2001 PNNL-13744.
26. Trivelpiece C, Jantzen C, Crawford C. Accelerated Leach Testing of GLASS: ALTGLASS Version 3.0. SRS, 2016 SRNL-STI-2016-00527, Rev. 0.
27. Bansal N, Doremus R. *Handbook of Glass Properties*. Orlando, FL: Academic Press, Inc.; 1986.
28. Jantzen C, Pickett J, Brown K, Edwards T, Beam D. Process/Product Models for the Defense Waste Processing Facility (DWPF): Part I. Predicting Glass Durability from Composition Using a Thermodynamic Hydration Energy Reaction Model (THERMO). 1995 WSRC-TR-93-672, Rev. 1.
29. Johnson F, Edwards T, Fox K. The User Guide for the ComPro™ Database. Savannah River National Laboratory, 2013 SRNL-STI-2009-00093, Rev. 1.
30. Johnson F, Edwards T, Fox K. Data Qualification Report: SRNL Glass Composition - Properties (ComPro™) Database. Savannah River National Laboratory, 2013 SRNL-STI-2009-00094, Rev. 1.
31. Knoche R, Dingwell D, Webb S. Melt densities for leucogranites and granitic pegmatites: Partial molar volumes for SiO₂, Al₂O₃, Na₂O, K₂O, Li₂O, Rb₂O, Cs₂O, MgO, CaO, SrO, BaO, B₂O₃, P₂O₅, F₂O₋₁, TiO₂, Nb₂O₅, Ta₂O₅, and WO₃. *Geochimica et Cosmochimica Acta*. 1995;59(22):4645-52.
32. McClane D, Amoroso J, Fox K, Kruger A. Nepheline crystallization behavior in simulated high-level waste glasses. *Journal of Non-Crystalline Solids*. 2019;505(1):215-24.

33. Morey G, Merwin H. The relation between the composition and the density and optical properties of glass. I. The soda-lime-silica glasses. *Journal of the Optical Society of America*. 1932;22(11):632-62.
34. Rao B. Influence of TiO₂ on properties of glasses in the system K₂O–PbO–SiO₂–TiO₂ and its relation to structure. *Journal of the American Ceramic Society*. 1963;46(3):107-14.
35. Tsujimura T, Xue X, Kanzaki M, Walter M. Sulfur speciation and network structural changes in sodium silicate glasses: Constraints from NMR and Raman spectroscopy. *Geochimica et Cosmochimica Acta*. 2004;68(24):5081-101.
36. Skidmore C, Vienna J, Jin T, Kim D, Stanfill B, Fox K, et al. Sulfur Solubility in Low Activity Waste Glass and its Correlation to Melter Tolerance. *International Journal of Applied Glass Science*. 2019;00:1-11. <https://doi.org/0.1111/ijag.13272>.
37. Bingham P, Vaishnav S, Forder S, Scrimshire A, Jaganathan B, Rohini J, et al. Modelling the sulfate capacity of simulated radioactive waste borosilicate glasses. *Journal of Alloys and Compounds*. 2017;695:656-67.
38. Mysen B, Cody G, Smith A. Solubility mechanisms of fluorine in peralkaline and meta-aluminous silicate glasses and in melts to magmatic temperatures. *Geochimica et Cosmochimica Acta*. 2004;68(12):2745-69.
39. Baasner A, Schmidt B, Dupree R, Webb S. Fluorine speciation as a function of composition in peralkaline and peraluminous Na₂O–CaO–Al₂O₃–SiO₂ glasses: A multinuclear NMR study. *Geochimica et Cosmochimica Acta*. 2014;132:151-69.
40. Hill R, Wood D, Thomas M. Trimethylsilylation analysis of the silicate structure of fluoro-alumino-silicate glasses and the structural role of fluorine. *Journal of Materials Science*. 1999;34(8):1767-74.
41. Dingwell D, Knoche R, Webb S. The effect of F on the density of haplogranite melt. *American Mineralogist*. 1993;78(3-4):325-30.
42. Hanifi A, Genson A, Pomeroy M, Hampshire S. Independent but additive effects of fluorine and nitrogen substitution on properties of a calcium aluminosilicate glass. *Journal of the American Ceramic Society*. 2012;95(2):600-6.
43. Ramos A, Levelut C, Petiau J. Local environment of selenium in silicate glasses. *Journal of Non-Crystalline Solids*. 1992;151(1-2):13-22.
44. Bingham P, Connelly A, Cassingham N, Hyatt N. Oxidation state and local environment of selenium in alkali borosilicate glasses for radioactive waste immobilisation. *Journal of Non-Crystalline Solids*. 2011;357(14):2726-34.
45. Volf M. *Chemical Approach to Glass*. Amsterdam: Elsevier Science Publishing Company, Inc; 1984.
46. *Handbook of Chemistry and Physics 2018* [cited 2019 February 26, 2019]. Available from: <http://hbcponline.com/faces/contents/InteractiveTable.xhtml?search=true&tableId=15>.
47. Johnson FC, Edwards TB. Selection of glasses in support of the Sludge Batch 9 variability study for coupled operation with the Salt Waste Processing Facility. United States: 2019 2019-03-08.
48. Fox K, Tommy Edwards T, David Peeler D. HIGH LEVEL WASTE (HLW) SLUDGE BATCH 4 (SB4): SELECTING GLASSES FOR A VARIABILITY STUDY. United States: pubinfo, 2006 2006-08-17.

Table 1: The partial molar volumes applied to the oxides in the database. The bound molar volume, v_i , is simply determined by dividing the molar weight of the oxide by the bound density given in Volf [13]. For the oxides which have “bound molar volume” values, the free molar volume is given in parentheses.

Oxide	Partial Molar Volume (cm ³ /mol)	Oxide	Partial Molar Volume (cm ³ /mol)	Oxide	Partial Molar Volume (cm ³ /mol)
Al ₂ O ₃	40.78 (25.55)	Fe ₂ O ₃	31.20	SO ₃ , SO ₄ (as Na ₂ SO ₄) [†]	52.61
As ₂ O ₃	52.89	Gd ₂ O ₃	48.92	Sb ₂ O ₃	47.02 (51.69)
B ₂ O ₃	24.87 (27.30)	K ₂ O	33.64 (40.08)	Se (as SeO ₃ ²⁻) [‡]	36.91
BaO	21.91 (26.80)	La ₂ O ₃	50.05	SiO ₂	26.36 (27.31)
Bi ₂ O ₃	45.24 (52.35)	Li ₂ O	11.07 (14.84)	Sm ₂ O ₃	45.88
CaO	14.38 (16.79)	MgO	12.22 (11.20)	SrO	17.56 (22.05)
CdO	17.83 (15.75)	MnO	13.70	Ta ₂ O ₅	53.62
CeO ₂	23.60	MnO ₂	17.11	TeO ₂	27.05
Ce ₂ O ₃	46.90	MoO ₃	30.63	ThO ₂	31.81 (27.25)
CoO	13.20	Na ₂ O	20.00 (27.30)	TiO ₂	21.02 (20.80)
CrO ₃	37.00	Nd ₂ O ₃	46.48	Tl ₂ O	63.40 (41.62)
Cr ₂ O ₃	29.20	NiO	33.50	U ₃ O ₈	100.48
Cs ₂ O	63.00	P ₂ O ₅	59.50	UO ₂	24.80
CuO	12.40	PbO	22.32 (23.51)	UO ₃	39.20
Cu ₂ O	23.80	Pr ₂ O ₃	47.80	Y ₂ O ₃	46.70
F [‡]	14.20	Rb ₂ O	45.59 (46.74)	ZnO	14.53 (14.82)

[†] See “Assumption 1.”

[‡] See “Assumption 2.”

FeO	12.60	RuO₂	18.87	ZrO₂	23.25 (22.44)
------------	-------	------------------------	-------	------------------------	---------------

FIGURES & CAPTIONS:

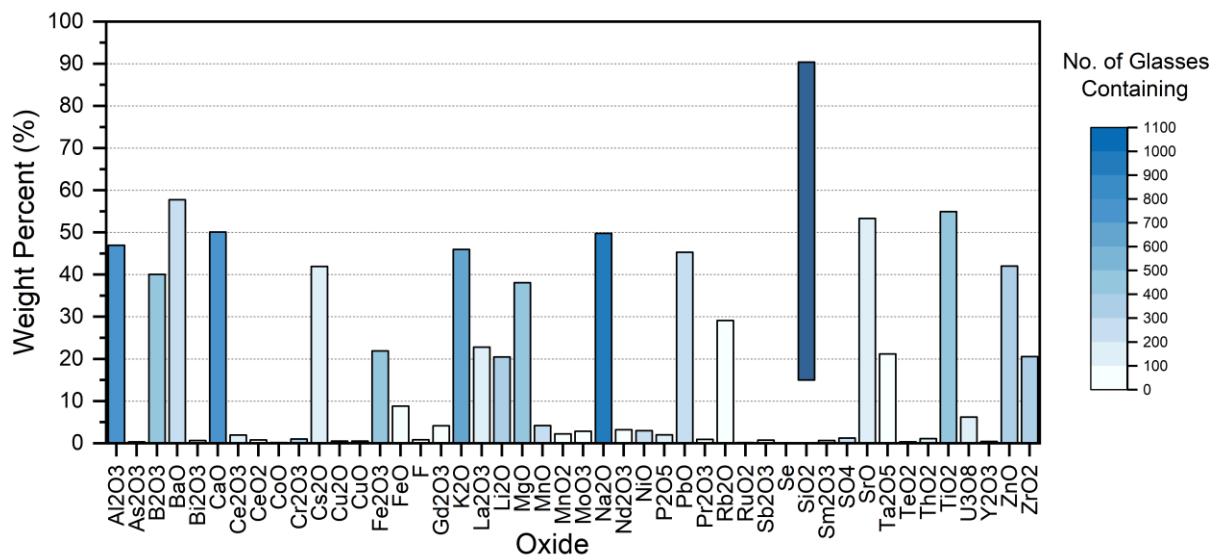


FIGURE 1. The compositional space covered by the glasses in the database. The colorbar represents the approximate number of glasses containing an oxide. The top and bottom represent the maximum and minimum concentration, respectively, of each oxide.

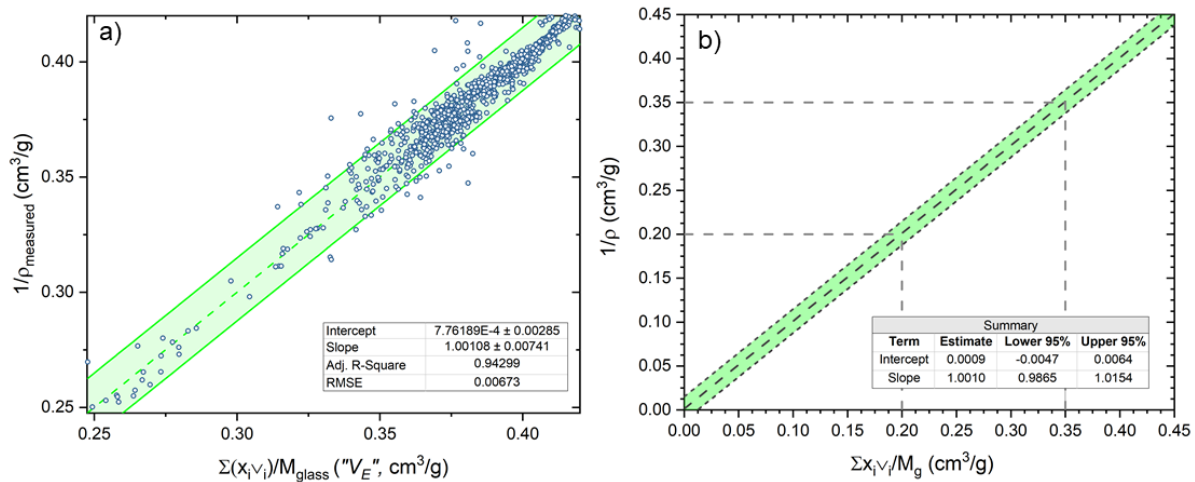


FIGURE 2. **(a)** The inverse measured density versus the estimated specific volume (V_E). The green shaded region represents the 95% tolerance level on the individual estimates. **(b)** The extension of the fit given by the dashed green line in (a) through the graph origin demonstrating an intercept of zero and a slope of one are contained within the tolerance interval.

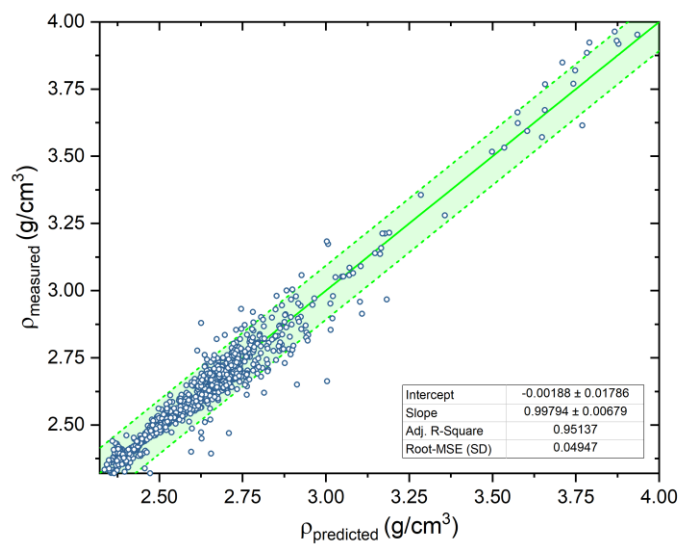


FIGURE 3. The measured glass density versus the inverse of the estimated specific volume for each glass. The green shaded region represents the 95% confidence interval on the individual predictions and the dashed green line is a linear fit of the estimated to the measured values.

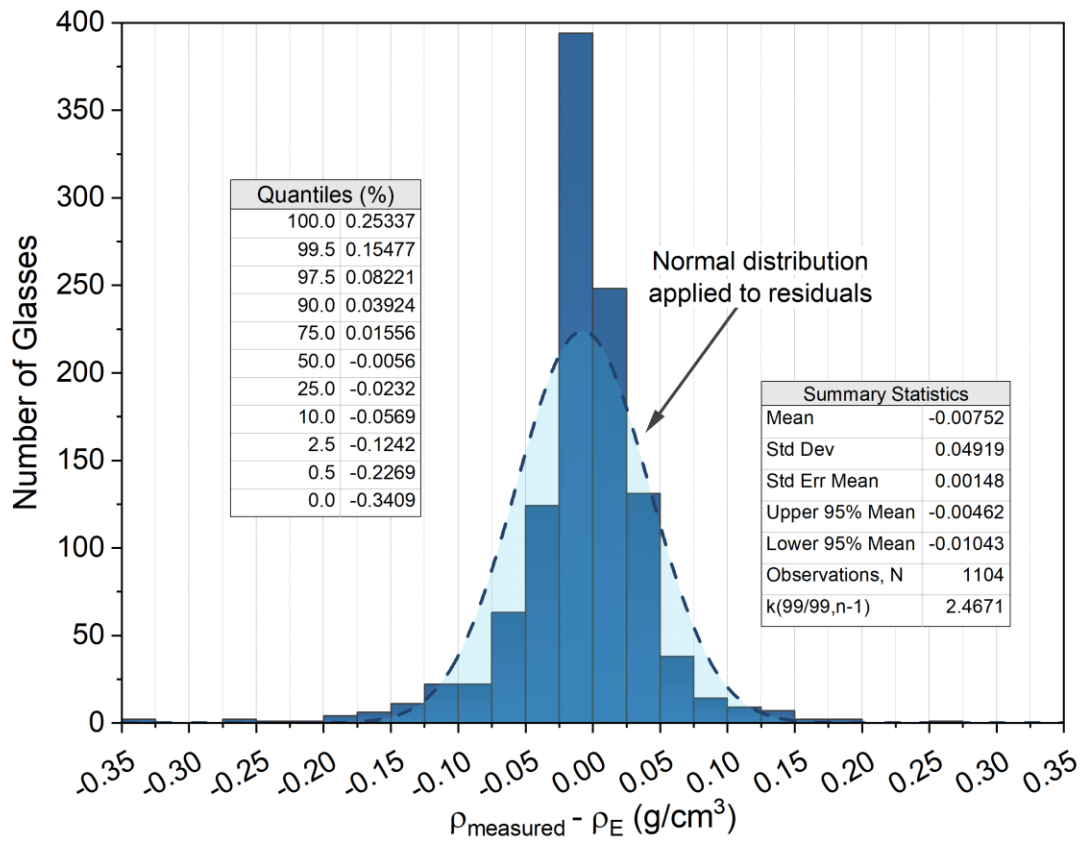


FIGURE 4. The histogram of the residual errors of individual estimates of glass densities in the database. The dashed line represents a normal distribution fitted to the residual data.

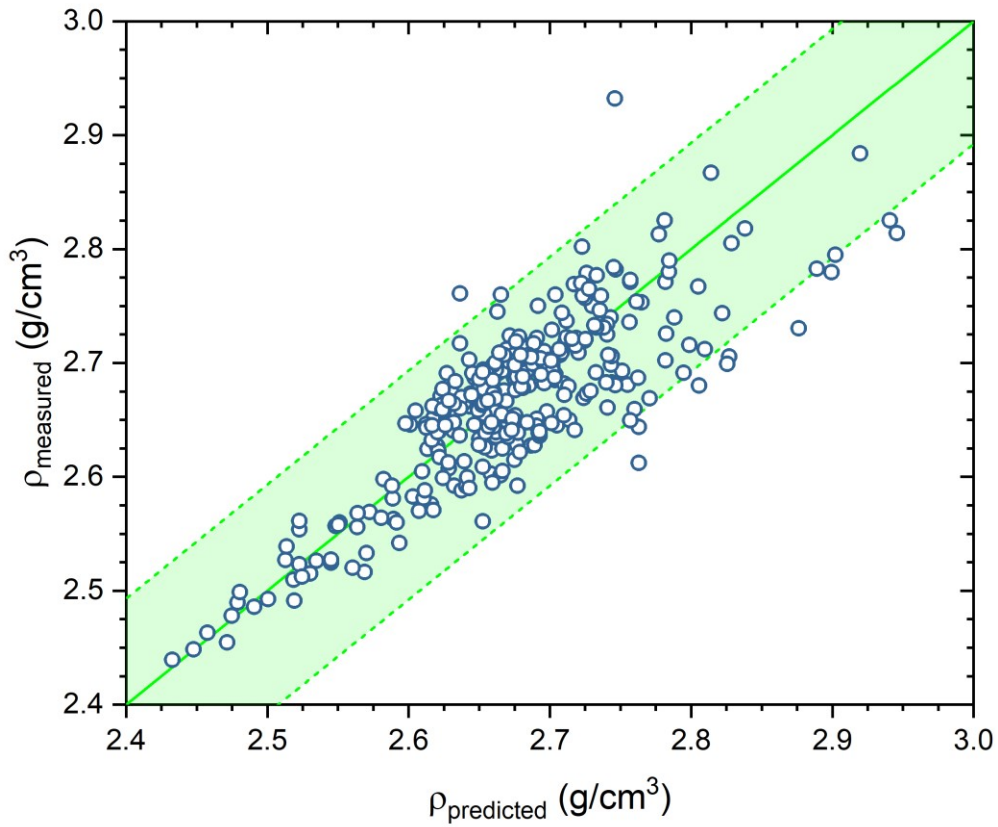


FIGURE 5. Estimated densities of a HLW glass subset from the database. The bound, shaded region demarcates the tolerance region for 95% coverage at 95% confidence. Fourteen glasses fall outside this region, which is approximately equal to 5% of the compositions in the subset.

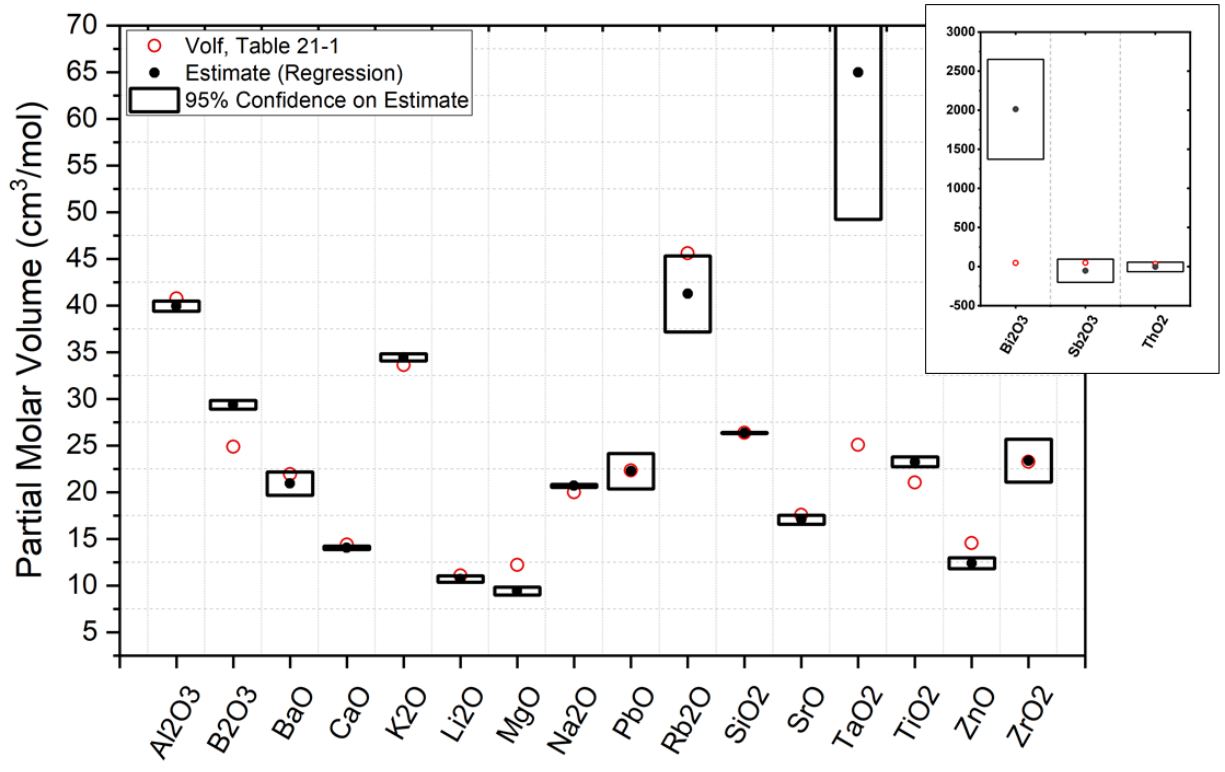


FIGURE 6. A comparison of some of the estimated partial molar volumes from the regression in Equation 5 with the values taken from Volf¹³ in Table 1. The inset graph shows the same information for three additional oxides.

